Spatial and Temporal Variability of Circulation Patterns within a Small Coastal Embayment During an Upwelling/Relaxation Cycle

A Senior Project
presented to
the Faculty of the Physics Department
California Polytechnic State University – San Luis Obispo

In Partial Fulfillment
of the Requirements for the Degree
Bachelor of Science in Physics

By

Laurent Siroit

June 2020

Approval Page

Title: Spatial and Temporal Variability of Circulation Patterns within a Small Coastal Embayment During an Upwelling/Relaxation Cycle

Author: Laurent Siroit

Date Submitted: 6/11/2021

Senior Thesis Advisor: Dr. Ryan Walter

_____

Signature

_____

Date

Contents

1 Introduction

Along eastern boundary currents, coastal upwelling is one of the dominant divers of physical, chemical, and biological variability (Checkley and Barth, 2009). Coastal upwelling is caused by equatorward winds that drive Ekman transport, or the offshore transport of surface waters offshore due to the Coriolis force. This generates a horizontal flux divergence of surface waters that requires a vertical flux of deeper waters into the nearshore. These deeper waters are nutrient rich and fuel photosynthesis and primary production in nearshore habitats. However, the upwelling process which relies on equatorward wind forcing is inherently variable. Along the California Current, seasonal upwelling winds are strongest during the major upwelling season (approximately April-September), although there is strong intraseasonal variability (García-Reyes and Largier, 2012; Walter et al. 2018). During the major upwelling season, strong upwelling events are typically followed by periods of wind relaxation, lasting several days, and thus are termed upwelling-relaxation cycles.

In coastal embayments along eastern boundary current upwelling systems, coastal upwelling variability is one of the dominant drivers of circulation patterns and variability, and thus have been termed “upwelling bays” (e.g., Largier 2020). In these upwelling bays, bathymetric and topographic variations have strong influences on upwelling-driven circulation patterns. For example, headlands can modify the alongshore airflow by either accelerating upwelling winds into an embayment or blocking upwelling winds and creating an “upwelling shadow” within the embayment (Largier, 2020). As noted by Largier (2020), the acuity, size, and orientation of topographic features all have significant influence on the circulation patterns present within coastal embayments. The shape of these embayments combined with the variability of upwelling-relaxation cycles, creates complex, time-dependent circulation patterns

(e.g., Shulman et al. 2009). These complex circulation patterns can have large impacts on the dispersal, retention, and connectivity of larval fish and invertebrate populations. For example, Roughan et. al. (2005) observed greater settlement of planktonic organisms within a small upwelling bay in the lee of a small headland (Bodega Bay, California) at the onset of upwelling favorable conditions. Additionally, circulation patterns in smaller upwelling bays also effect localized upwelling (Walter et. al. 2017) and the development and transport of harmful algal blooms (Ryan et al. 2008), both of which have significant implications for biogeochemical variability. While steady-state descriptions of circulation patterns exist for upwelling and downwelling forcing in upwelling bays (e.g., Paduan et al. 2016; Trautman, 2020), time-dependent descriptions of complex circulation patterns during upwelling/relaxation cycles are sparse, particularly for small coastal embayments [i.e., length and width scales less than 20 km, see e.g., Largier (2020)].

In this study, we investigate the temporal variability of circulation patterns in a small coastal embayment located in Central California [San Luis Obispo (SLO) Bay]. A past study on SLO Bay by Trautman (2020) focused on the seasonal, steady-state, surface current patterns during upwelling and downwelling forcing, calculated through a process of conditional averaging (cf. Paduan et. al. 2016). Here we focus on the spatial and temporal variability of an upwelling-relaxation cycle. Both surface currents and subsurface currents are used to discern the circulation patterns in and around SLO Bay. We also highlight the importance of spatiotemporal surface current patterns through the use of a particle tracking model. Implications of the findings are discussed.

2 Data and Methods

2.1 Description of Study Site

SLO Bay (Figure 1) is a small semi-enclosed coastal embayment (width and length scales $\leq$ 20 km), as characterized by Largier (2020). It is located along the central California coast, between Point San Luis to the north and Point Sal to the south. Mountainous terrain north of the bay, including Mt. Buchon (~550 m tall), shelters the northern most part of the bay from northwesterly winds. These conditions result in an "upwelling shadow" system with warmer waters in the bay shadow, which affects bay biogeochemistry and circulation patterns within the bay (Walter et al, 2018). SLO Bay is also an ecologically diverse habitat which features large kelp forests, and it is home to the Harford pier, a commercial fishing port, and the California Polytechnic (Cal Poly) State University Pier. SLO Bay is also prone to harmful algal blooms (Barth et al. 2020) and hypoxic events (Valera et a. 2020).

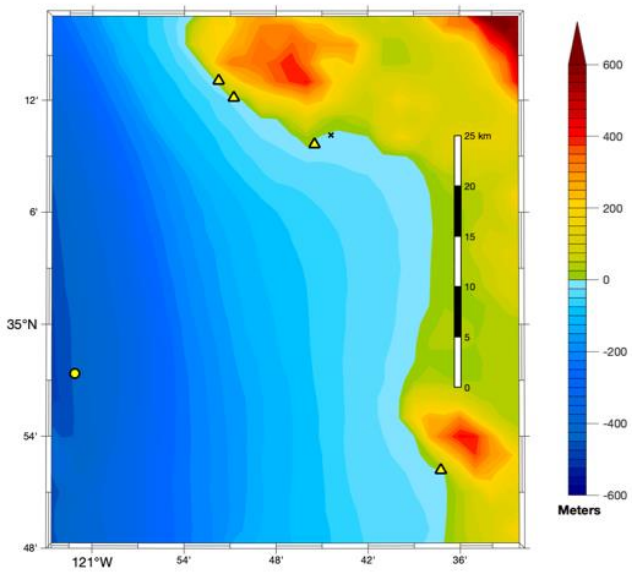

Figure 1. Bathymetry and topography around the San Luis Obispo Bay. Locations of NDBC Buoy #46011 and HFR sites are shown as a yellow circle and yellow triangles, respectively. A bottom-mounted mooring for nearshore subsurface velocity profile measurements, located at the end of the Cal Poly Pier, is shown as a black "x".

2.2 Surface Current Data

A network of High Frequency Radar (HFR) antennas employs backscattered radio signals to remotely measure ocean surface currents. Surface waves with wavelengths equaling half the radar wavelength will backscatter the emitted radar signal and result in a strong return signal, a phenomenon known as Bragg scattering. Differences between the predicted backscattered frequency of surface waves and the actual backscattered frequency are caused by surface currents (Paduan et. al. 2012). The Doppler shift caused by the underlying surface currents is then used to measure surface currents up to 200 km offshore at varying spatial resolution depending on the radar frequency. HFR data with a spatial resolution of 2 km and a temporal resolution of 1 hr were obtained from HFRNet (https://hfrnet- tds.ucsd.edu/thredds/catalog.html).

2.3 Subsurface Current Data

To investigate nearshore subsurface currents in SLO Bay, we utilized data from an upward looking Nortek Acoustic Wave and Current Profiler (AWAC) moored ~20 m off the end of the Cal Poly Pier (Figure 1). In order to measure velocities at various depths (bins) throughout the entire water column, this technology transmits bursts of high frequency acoustic waves through the water column. The sound waves bounce off suspended particles and are reflected back towards the instrument. The reflected waves will have a slightly lower frequency when reflected off particles moving away from the instrument, and a slightly higher frequency for particles moving toward the instrument. The difference in frequency of the emitted and received signals, or the Doppler Shift, is then used to calculate the velocities at various bins throughout the above water column.

2.4 Offshore Wind Data

Hourly offshore wind measurements were obtained from the National Data Buoy Center (NDBC) Buoy # 46011, which is located approximately 35 km offshore of SLO Bay (Figure 1). Equatorward upwelling favorable winds were calculated such that they are parallel to the local coastline (150° from true north; Figure 1, Walter et al., 2018). Positive values indicate upwelling favorable winds and negative value indicate downwelling favorable winds.

2.5 Data Processing

The time period of interest was the full upwelling seasons from March to September 2016, which includes the previously defined Peak Upwelling season (April, May), the Upwelling Relaxation season (July-Sept), and the Upwelling Transition periods (March, June) for this region (Walter et. al 2018). The timestamps of the upwelling winds were interpolated onto the HFR surface current timestamps so that they could be correlated. Additionally, the upwelling winds, HFR surface current, and subsurface current timeseries were filtered using a 33 hr low-pass filter in order to focus on the upwelling-relaxation wind-driven circulation and to remove higher frequency variability caused by tides and local diurnal wind forcing (e.g., Walter et al. 2017). The horizontal divergence of the surface current velocity field was calculated for a region around the mouth of the bay. From the calculated divergence, the mean divergence (and standard deviation) were obtained. A lagged cross-correlation analysis was also performed between the divergence at individual points and the upwelling winds.

2.6 Particle Tracking Algorithm

A particle tracking algorithm, originally developed by researchers at the University of California Santa Barbara (UCSB) for HFR data (e.g., Emery et al. 2019), was used to study particle trajectories. In order to calculate trajectories, the algorithm requires a velocity field

which is gap free in both time and space. This algorithm employs empirical orthogonal functions (EOF) to fill in data gaps and particles are advected using a fourth-order Runge-Kutta Method.

3 Results

3.1 Seasonal Upwelling Circulation Patterns

The mean surface currents across the full upwelling season showed a strong upwelling jet forming across the mouth of SLO Bay which advects onto the shore in the southern portion of the bay (Figure 2a). The mean horizontal divergence revealed a strong convergence which forms at the mouth, where waters from within the northern part of the bay moved offshore and met the upwelling jet (Figure 2a). The location of this convergence zone matched the location of the upwelling shadow front [see e.g. Figure 9 in Walter et. al (2018)]. There was also a region of strong divergence near the southern end of the bay. Both the strong convergence and divergence regions in the northern and southern portion of the bay, respectively, were highly variable (Figure 2b).

The cross-correlation analysis between the upwelling favorable winds and the horizontal divergence field revealed a strong negative correlation in the northern convergence zone (Figure 3a). Additionally, there was little to no lag between the upwelling favorable winds and the formation of the convergence zone at the northern mouth of the bay (Figure 3b).

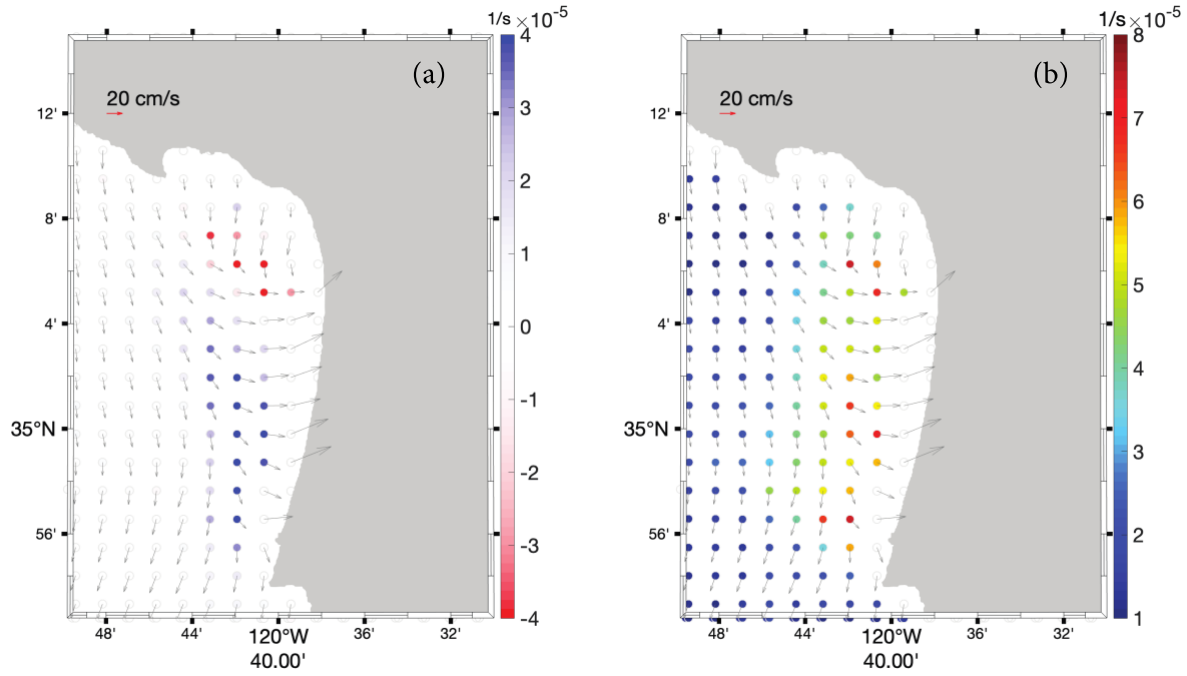

Figure 2. (a) Mean and (b) standard deviation of the horizontal divergence field in SLO bay calculated from surface currents during the full 2016 upwelling season (March to September).

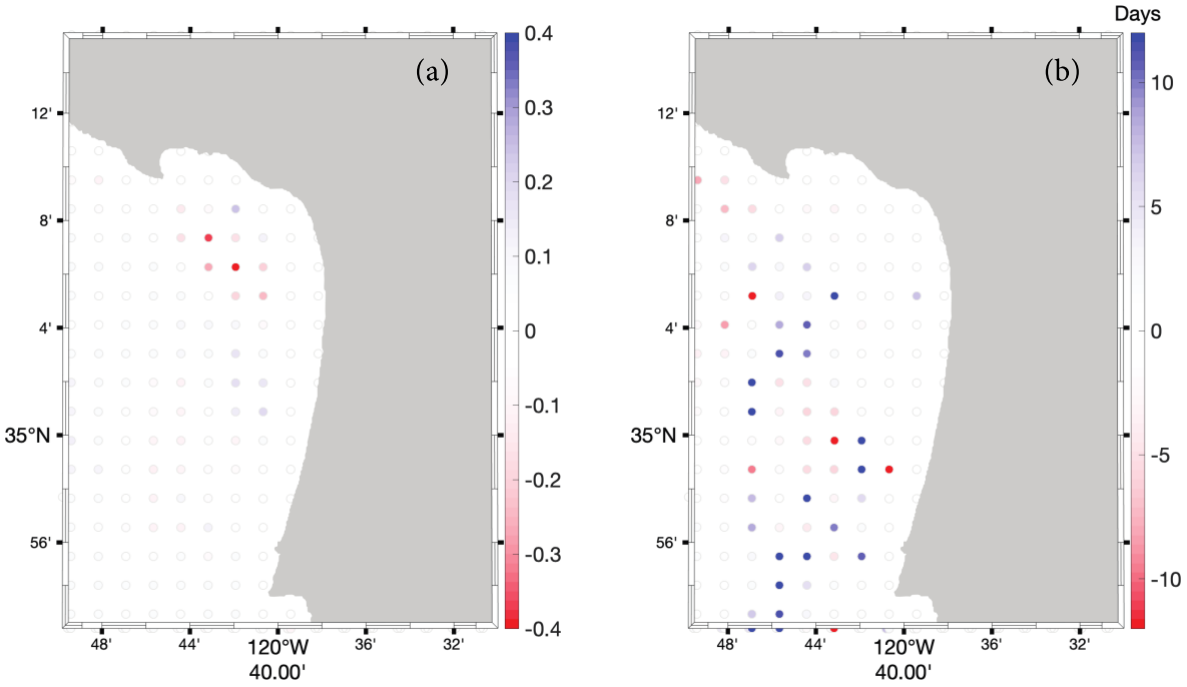

Figure 3. (a) Cross-correlation between horizontal divergence field and upwelling winds with (b) the associated lag time for the full 2016 upwelling season (March to September).

3.2 Spatial and Temporal Circulation Patterns of an Upwelling-Relaxation Event

A 12-day upwelling-relaxation cycle was examined to investigate the detailed temporal and spatial evolution of the convergence zone at the northern mouth of the bay. An upwelling jet began to form north of the bay over the 2-day period from April 10th to 12th (Figure 4b) when upwelling winds started to increase from zero (i.e., the previous relaxation event; Figure 4a). Over the next two days (April 14th to April 16th), the upwelling jet strengthened and advected towards the shore in the southern part of the bay as the upwelling favorable winds continued to increase (Figure 4c). Following this, the upwelling winds peaked and started to subside over the 2-day period from April 14th to 16th. During this time, the onshore advection in the southern bay ceased and the upwelling jet reattached to the offshore upwelling jet (Figure 4d). Due to the evolution of the upwelling jet across the mouth of the bay, there was a strong convergence zone across the entire mouth of the bay when the upwelling jet advected onshore from April 12th to 14th. The strength of the convergence zone at the mouth of the bay reached its peak only after the upwelling winds surpassed 5m/s. From April 14th to 16th, the convergence zone in the southern portion of the bay dissipated while the convergence zone at the northern mouth of the bay persisted.

During this event, the particle tracking model showed that particles released on April 8th and 10th, before the convergence zone had fully formed, were advected offshore and to the south of the embayment (Figure 5 a-h). On April 12th, and once the upwelling wind surpassed 5 m/s, the particles got trapped in the strong convergence zone and all of them were retained in the nearshore (i.e., defined here as when the particles advected out of the gridded velocities inside the embayment) (Figure 5 i-l). From April 14th to 16th, some particles were retained in the

embayment and advected out of the gridded velocities on the nearshore side while others advected south as the upwelling jet reattached to the offshore equatorward flow (Figure 5 m-t).

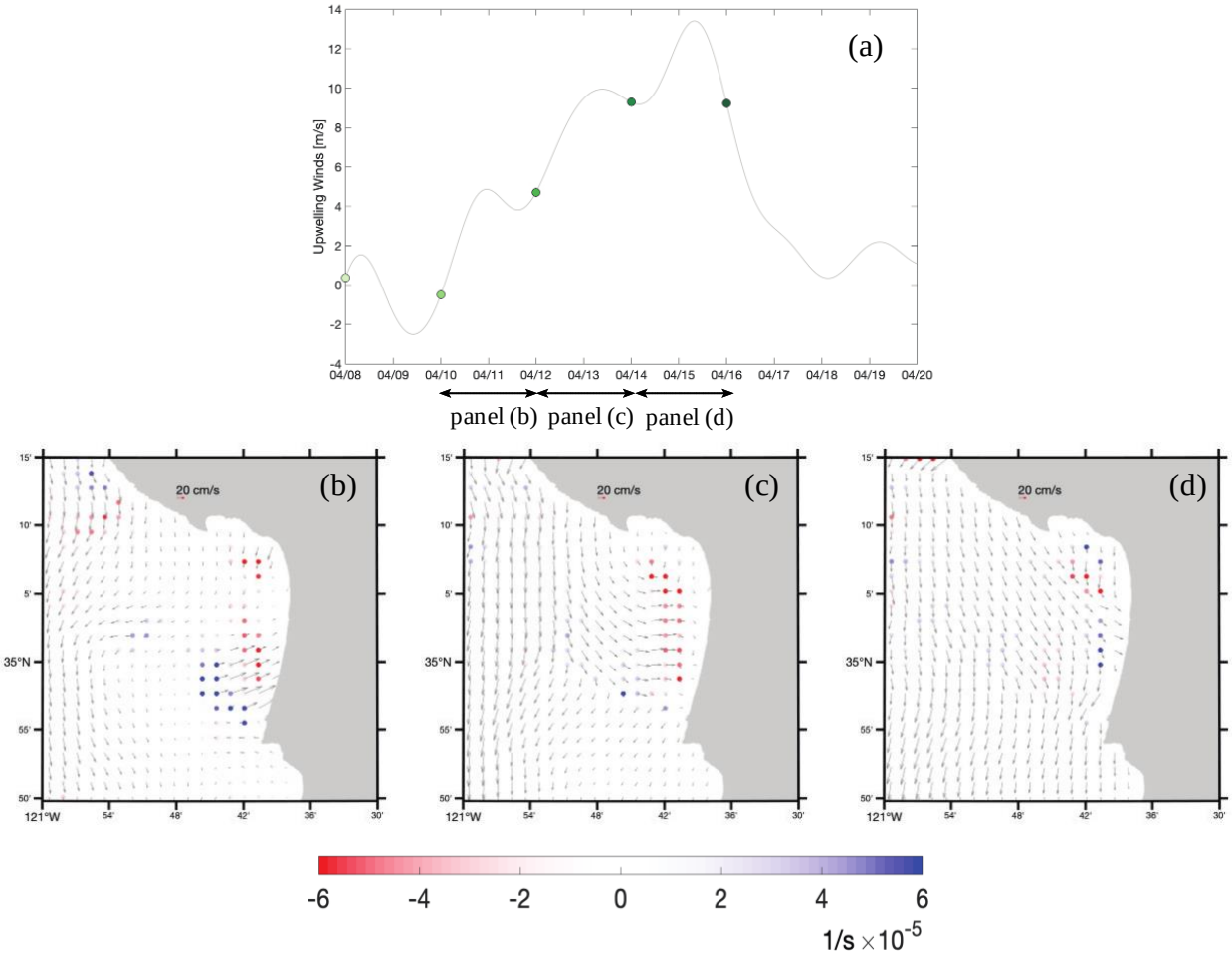

Figure 4. (a) Time series of upwelling favorable winds during a 12-day upwelling-relaxation cycle in April 2016. Colored circles indicate times at which particles are released in the particle tracking model with the color matching the corresponding particles in Figure 5. (b-d) Time-averaged divergence field overlaying the average surface currents for a 2-day period (2-day period shown on bottom of panel a).

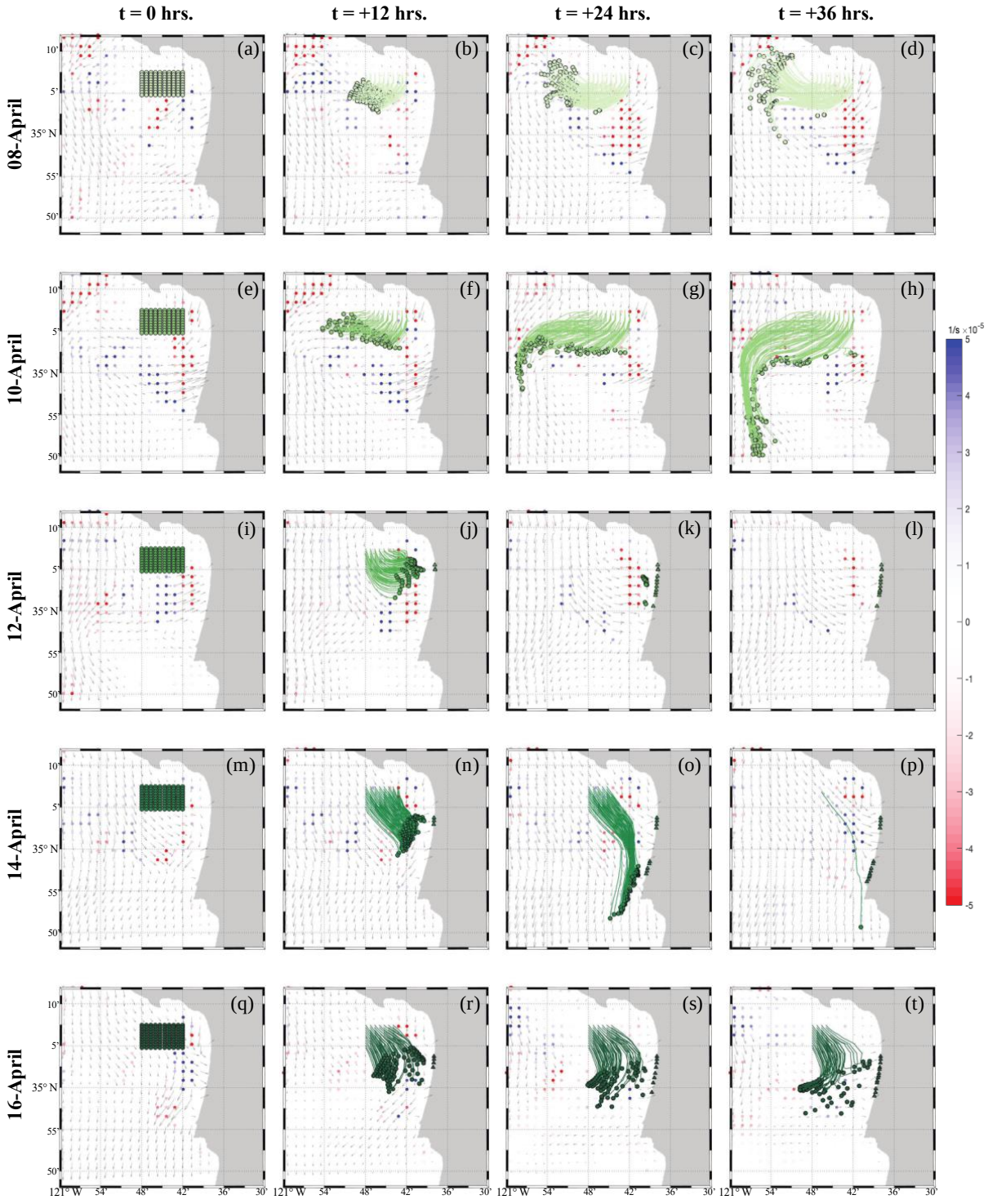

Figure 5. Particle tracks for 100 particles released every 48 hrs., beginning on April 8th at 00:00 and ending on April 16th at 00:00 (see Figure 4). Snapshots of the particle tracks are shown every 12 hrs. Triangles represent particles which are retained inside the bay (i.e., advect out of the gridded velocities of the nearshore side). Each panel shows the horizontal divergence field overlaying the surface current field for that time point.

3.3 Subsurface Circulation Patterns of An Upwelling-Relaxation Cycle

Subsurface current velocities (Figure 6b,c) within the northern portion of the bay varied throughout the water column. From April 10th to 15th, while upwelling favorable winds were positive and increasing, waters in the bottom-most layer moved consistently in a southwestern direction or out of the bay. Once upwelling favorable winds reached 5 m/s on April 12th, waters in the middle of the water column moved in a northeastern direction, or into the bay. However, the middle layer experienced a brief period of western flow from April 14th to 15th when upwelling winds briefly stopped increasing. The top-most layer consistently moved southeast, or into the southern portion of the bay.

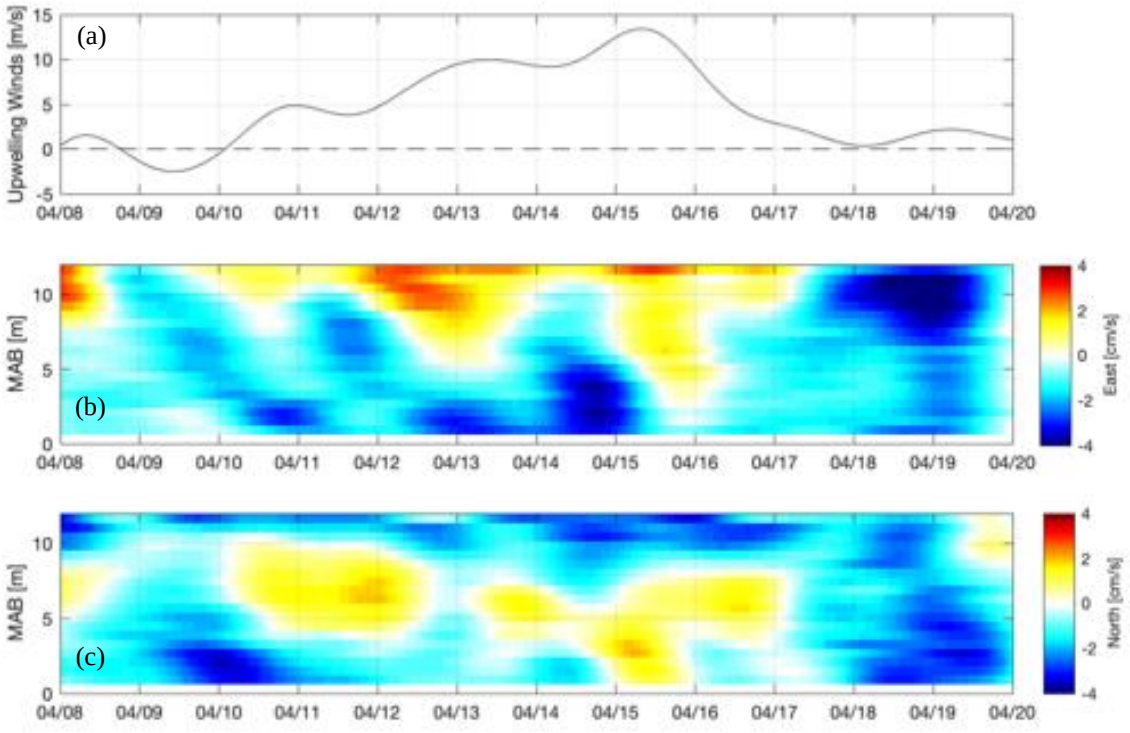

Figure 6. Time series over 12-day period in April 2016 of the (a) upwelling favorable winds, as well as the (b) east/west and (c) north/south nearshore velocities throughout the water column.

4 Discussion

4.1 Transient Upwelling-Relaxation Circulation Patterns

The quasi-steady state circulation patterns during upwelling-relaxation events in SLO bay have been well established. Using conditional averages of surface currents based on upwelling favorable winds, Trautman (2020) examined steady-state surface current circulation patterns which arise in SLO Bay. Their work detailed an upwelling jet that forms across the mouth of the bay, with significant onshore advection towards the southern end (Trautman 2020). Additionally, using the upwelling seasonality proposed by Walter et. al (2018), Trautman (2020) found that upwelling events occurring during the Peak Upwelling season (April and May) appeared to contribute more to the observed circulation patterns than upwelling events occurring during the Upwelling Relaxation season (July to September). Building on this previous work, we examined the spin-up to this steady-state description using a large upwelling-relaxation event in the Peak Upwelling season. We found that once the upwelling winds reached a strength of 5 m/s, which took 2 days for this event (Figure 4a.), the upwelling jet was fully formed and advected towards the southern end of the bay. The jet reattached on April 16th (Figure 5q.) when upwelling winds began to dissipate. Moreover, the subsurface response showed that once upwelling winds reached 5 m/s, the surface layer of waters inside the bay consistently moved southeast (into the convergence zone) while the bottom and middle layers moved northwest (into the northern portion of the bay) (Figure 6). Once upwelling winds decreased below 5 m/s and the surface convergence zone dissipated on April 17th (Figure 5s), the water mass inside the bay moved southwest (out of the bay) (Figure 6).

Despite their ubiquity, small embayments (length and width scale $\leq$ 20 km) are relatively understudied (Largier 2020). Due to the large prevalence of small embayments in eastern

boundary current upwelling systems, a deeper understanding of the complex circulation patterns present in SLO bay could serve as a baseline for the understanding of circulation patterns in other small upwelling bays. The northern region of SLO Bay is sheltered from upwelling favorable winds due a large headland, a characteristic feature of "upwelling shadow" systems. The local coastal orientation and topographic features result in the development of a retention zone and a strong front which separates warmer waters inside the bay from the colder waters which extend across the mouth of the bay (Walter et. al. 2018). Trautman (2020) found that the strong front at mouth of the bay coincided with the region of enhanced surface current convergence observed during the Peak Upwelling and Upwelling Relaxation seasons and proposed that the upwelling jet and shoreward circulation comprise a positive feedback mechanism by which the upwelling shadow and front are reinforced. The transient circulation patterns during an upwelling-relaxation cycle investigated in this study further support this proposed mechanism. Mechanistically, as the upwelling wind forcing increases, offshore Ekman transport lowers the sea surface level near the coast and causes the thermocline to shoal towards the surface. This cross-shelf pressure gradient results in a well-established and documented along-shore geostrophic flow ("jet") (Largier 2020). Due to the presence of a headland, this upwelling jet separates from the coast at the northern end of SLO Bay and advects towards the southern shore of the bay. The separated upwelling jet traps a warm surface layer inside the bay which increases the baroclinic pressure gradient force and reinforces the surface convergence zone along the front (Trautman 2020). However, following a decrease in the upwelling wind on April 16th, which occurred approximately 5 days after the start of the upwelling event, the separated jet reattached to the main jet and no longer advected onshore in the southern end of the bay (Figure 5q). Following this, the region of enhanced surface current convergence began to

dissipate around April 17th (Figure 5s). While this study highlights important details of the time-dependence of the mechanism first proposed in Trautman (2020), more realizations are required to fully characterize the spin-up and evolution across different upwelling events and seasons.

4.2 Ecological Implications

The formation and reinforcement of an upwelling shadow front in SLO Bay by complex surface circulation may increase the retention of planktonic species within the bay. The region of strong surface current convergence that forms in the event described here took approximately 4 days to reach peak convergence and then persisted for another 4 days (Figure 5). During this period, increased retention was observed (Figure 6). The increased retention in SLO Bay due to complex circulation patterns observed should be considered, in addition to changing environmental conditions (e.g., nutrient fluxes, stratification, mixing, etc.), when assessing phytoplankton community composition, including the formation and persistence of harmful algal blooms (Barth et. al 2020), as well as nearshore hypoxia (Valera et. al 2020). Future work should assess how variable upwelling forcing (i.e., magnitude and duration of event) impacts retention time and the resulting ecological ramifications.

5 Conclusion

In eastern boundary current systems, wind-driven coastal upwelling is the dominant diver of physical, chemical, and biological variability. Near coastal embayments, complex circulation patterns develop during upwelling forcing, and time-dependent descriptions of these patterns for smaller systems (i.e., width and length scales $\leq$ 20 km) are limited. In this study, we analyze surface and subsurface current patterns in relation to upwelling wind forcing in San Luis Obispo (SLO) Bay, a small coastal upwelling embayment in central California, to investigate the

formation and evolution of an upwelling jet and surface current convergence region during a large upwelling-relaxation event. We found that the offshore upwelling jet advected onshore once the upwelling winds reached 5 m/s, and this coincided with the formation of a strong surface convergence region across the mouth of the bay. A particle tracking model revealed enhanced nearshore retention of particles released at the surface following the formation of a strong convergence region. Once the upwelling winds decreased, the upwelling jet reattached to the offshore equatorward jet and the convergence region decreased substantially. When the upwelling winds decreased to below 5 m/s, the convergence zone fully dissipated and the water mass inside the bay was flushed out. The formation, evolution, and persistence of the convergence zone at the mouth of SLO Bay has important biological and ecological implications; however, more realizations are required to fully characterize the spin-up and evolution across different upwelling events and seasons.

6 Acknowledgements

We acknowledge support from the NOAA IOOS program through SCCOOS for the HF radar measurements, as well as past PIs and technicians that helped maintain these systems, especially Ian Robbins. Support for the AWAC measurements at the Cal Poly Pier was provided by CeNCOOS. We are grateful to Libe Washburn and Li Kui for sharing their most recent version of the particle tracking code originally developed by Emery et al. (2019). Foremost, I want to express my immense gratitude to my advisor, Dr. Ryan Walter, for his guidance and support. The knowledge and advice, both academic and personal, from Dr. Walter, will continue to guide me in my future endeavors.

References

Barth, A., Walter, R. K., Robbins, I., & Pasulka, A. (2020). Seasonal and interannual variability of phytoplankton abundance and community composition on the Central Coast of California. *Marine Ecology Progress Series*, *637*. https://doi.org/10.3354/meps13245

Checkley, D. M., & Barth, J. A. (2009). Patterns and processes in the California Current System. *Progress in Oceanography*, *83*(1–4). https://doi.org/10.1016/j.pocean.2009.07.028

Emery, B., Letcheronongguong, K., Ireson, K., Gotschalk, C., Ohlmann, C., & Washburn, L. (2019). Drifter Simulation Toolbox for MATLAB. https://doi.org/10.5281/zenodo.3350830

García-Reyes, M., & Largier, J. L. (2012). Seasonality of coastal upwelling off central and northern California: New insights, including temporal and spatial variability. *Journal of Geophysical Research: Oceans*, *117*(3). https://doi.org/10.1029/2011JC007629

Largier, J. L. (2020). Upwelling Bays: How Coastal Upwelling Controls Circulation, Habitat, and Productivity in Bays. In *Annual Review of Marine Science* (Vol. 12). https://doi.org/10.1146/annurev-marine-010419-011020

Paduan, J. D., Cook, M. S., & Tapia, V. M. (2018). Patterns of upwelling and relaxation around Monterey Bay based on long-term observations of surface currents from high frequency radar. *Deep-Sea Research Part II: Topical Studies in Oceanography*, *151*. https://doi.org/10.1016/j.dsr2.2016.10.007

Paduan, J. D., & Washburn, L. (2013). High-frequency radar observations of ocean surface currents. *Annual Review of Marine Science*, *5*. https://doi.org/10.1146/annurev-marine-121211-172315

Roughan, M., Mace, A. J., Largier, J. L., Morgan, S. G., Fisher, J. L., & Carter, M. L. (2005). Subsurface recirculation and larval retention in the lee of a small headland: A variation on the upwelling shadow theme. *Journal of Geophysical Research C: Oceans*, *110*(10). https://doi.org/10.1029/2005JC002898

Ryan, J. P., Gower, J. F. R., King, S. A., Bissett, W. P., Fischer, A. M., Kudela, R. M., Kolber, Z., Mazzillo, F., Rienecker, E. V., & Chavez, F. P. (2008). A coastal ocean extreme bloom incubator. *Geophysical Research Letters*, *35*(12). https://doi.org/10.1029/2008GL034081

Shulman, I., Anderson, S., Rowley, C., Derada, S., Doyle, J., & Ramp, S. (2010). Comparisons of upwelling and relaxation events in the Monterey Bay area. *Journal of Geophysical Research: Oceans*, *115*(6). https://doi.org/10.1029/2009JC005483

Valera, M., Walter, R. K., Bailey, B. A., & Castillo, J. E. (2020). Machine learning based predictions of dissolved oxygen in a small coastal embayment. *Journal of Marine Science and Engineering*, *8*(12). https://doi.org/10.3390/jmse8121007

Walter, R. K., Armenta, K. J., Shearer, B., Robbins, I., & Steinbeck, J. (2018). Coastal upwelling seasonality and variability of temperature and chlorophyll in a small coastal embayment. *Continental Shelf Research, 154*. https://doi.org/10.1016/j.csr.2018.01.002

Walter, R. K., Reid, E. C., Davis, K. A., Armenta, K. J., Merhoff, K., & Nidzieko, N. J. (2017). Local diurnal wind-driven variability and upwelling in a small coastal embayment. *Journal of Geophysical Research: Oceans*, *122*(2). https://doi.org/10.1002/2016JC012466